

High Order Finite Differencing Schemes and Their Accuracy for CFD

Yiqing Shen* Gecheng Zha†
Dept. of Mechanical and Aerospace Engineering
Miami Wind TM
University of Miami
Coral Gables, Florida 33124
E-mail: yqshen@miami.edu, gzha@miami.edu

Abstract

This paper investigates different high order finite difference schemes and their accuracy for Burgers equation and Navier-Stokes equations. On a coarse grid, theoretical and numerical analysis indicate that a higher order difference scheme does not necessarily obtain more accurate solutions than a lower order scheme in the regions of high gradient variation (2nd order derivative). On a coarse grid, the numerical experiments indicate that the 3rd order biased upwind differencing for the inviscid fluxes with 2nd order central differencing for viscous term outperforms all other schemes with the accuracy order as high as 7th order. For the linear Burgers equation, both the analytical and numerical results indicate that a higher order scheme will be more accurate than a lower order scheme only when $Re\Delta x \leq 1$. For the nonlinear Burgers equation, the numerical experiments also show the same conclusion.

A numerical solution of laminar wall boundary layer from Navier-Stokes equations shows the same observation that a lower order scheme is more accurate on a coarse grid. The conception that a high order scheme can reduce mesh size unconditionally may be incorrect. Since the discrepancy occurs mostly in the region with high gradient variation, the refined mesh should not only be near the wall surface where the gradient is high, but also near the edge of the boundary layer where the gradient variation is high. The mesh spacing criterion for Navier-Stokes equation that a higher order scheme will be more accurate than a lower order scheme is not obtained yet. Using the criterion of the linear Burgers equation for Navier-Stokes equations may be excessive and preventively expensive. To resolve a laminar wall boundary layer accurately, the recommended grid Reynolds number is to be below 25 across the boundary layer. However, this is the criterion from the numerical experiments for all the finite differencing schemes, not for the higher order schemes to have better accuracy.

1 Introduction

Developing high order numerical schemes has attracted a lot of attention recently in computational fluid dynamics for two expected advantages: First, high order schemes can resolve more detailed flow structures than a low order scheme based on the same mesh size. Second, to achieve the same resolution of a flow field, a high order scheme can use a smaller mesh size than a low order scheme and hence may save CPU time. An excellent review of recently developed high-order accurate finite-difference, finite-volume, and finite-element methods is given by Ekaterinaris[1]. Most of the research on high order schemes focus on

* Research Scientist, AIAA Member

† Associate Professor, AIAA Senior Member, Director of Miami Wind TM

the resolution of complex flowfield structures such as vortices interaction, vortex shear layers interaction, and shock capturing, etc.

CFD applications often need to treat wall boundary layer flows. The numerical simulation of a flow with only a wall boundary layer, which seems simple, is actually very challenging because of the existence of a large velocity gradient. A common conception is that a higher order accuracy finite differencing scheme can resolve the wall boundary layer with fewer grid points since the higher order scheme has less truncation error. In fact, such a conclusion is not necessarily true. It depends on the behavior of the solution.

For example, if a solution u has the form

$$u = e^{Re x},$$

where Re is a large number, such as a Reynolds number. The l th-derivative of u is

$$u^{(l)} = Re^l e^{Re x},$$

The truncation error of a finite differencing scheme based on Taylor's series expansion is determined by $\Delta x^l \cdot u^{(l)}/l!$, or $(\Delta x Re)^l/l!$. Even if the mesh interval is very small, $Re\Delta x$ may be still greater than 1 since R has a large value. When $Re\Delta x > 1$, the higher the order of a scheme, the larger the truncation error may be. Hence, it is not always true that a higher order scheme is more accurate than a lower order scheme. What is the condition that a higher order scheme will be more accurate? This issue has not been well addressed for CFD.

The object of this paper is to study different high order finite difference schemes and their accuracy for Burgers equation and Navier-Stokes equations by theoretical and numerical analysis. The results indicate that unless the mesh is sufficiently fine, the 3rd order biased upwind scheme for the inviscid flux with the 2nd order central differencing scheme outperforms all other schemes with the accuracy order as high as 7th order in the high gradient variation region. Please note the emphasis here is **high gradient variation** instead of only high gradient. The conception that the high order scheme is more accurate for Navier-Stokes may not be always true unless very fine mesh is used.

2 Theoretical Analysis

In this paper, only the central differencing and one-point-biased upwind differencing schemes are discussed.

For the approximation of derivative $\frac{\partial f}{\partial x}$ at node i , Taylor series expansion will give

$$\frac{\partial f}{\partial x}|_i = \frac{1}{\Delta x} \left[\sum_{k=m}^n c_k f_{i+k} + \sum_{l=n-m+1}^{\infty} D_l \frac{1}{l!} f_i^{(l)} \Delta x^l \right] \quad (1)$$

where $f^{(l)}$ is the l th-derivative of f . The first part of Eq.1 is the finite differencing scheme approximating the partial difference, and the second part is the truncation error of the approximation. The accuracy order of Eq. (1) is determined by the difference between n and m , $(n - m)$. For example, if $m = -2$ and $n = 1$, we will have a 3th-order biased differencing scheme. The coefficients c_k and D_l are given in Table1 and Table2 for different order schemes, respectively.

For a problem with the solution $f = f(Re x)$ (for example, the velocity distribution of boundary layer to be discussed later), the term Re^l will appear in the l th-derivative $f^{(l)}$. Hence, in Eq. (1), $\frac{D_l}{l!} f_i^{(l)} \Delta x^l$ can be replaced by $\frac{D_l}{l!} f_y^{(l)}|_i (Re\Delta x)^l$. In this paper, we only discuss the case of

$$f = f(y), \quad y = Re x. \quad (2)$$

Table 1: The coefficients of c_k

Scheme	f_{i-4}	f_{i-3}	f_{i-2}	f_{i-1}	f_i	f_{i+1}	f_{i+2}	f_{i+3}
2-order central				-1/2	0	1/2		
3-order biased			1/6	-1	1/2	1/3		
4-order central			1/12	-2/3	0	2/3	-1/12	
5-order biased		-1/30	1/4	-1	1/3	1/2	-1/20	
6-order central		-1/60	3/20	-3/4	0	3/4	-3/20	1/60
7-order biased	1/140	-1/15	3/10	-1	1/4	3/5	-1/10	1/105

Table 2: The coefficients of D_l

Scheme	D_3	D_4	D_5	D_6	D_7	D_8	D_9	D_{10}	D_{11}
2-order central	1		1		1		1		1
3-order biased		2	-4	10	-20	42	-84	170	-340
4-order central			-4		-20		-84		-340
5-order biased				-12	36	-168	504	-1764	5292
6-order central					36		504		5292
7-order biased						144	-576	4320	-17280

There are two facts for the solution of Eq. (2):

- (1) If $Re\Delta x$ is greater than 1, the larger the l , the greater the $(Re\Delta x)^l$.
- (2) $\lim_{l \rightarrow \infty} \frac{(Re\Delta x)^l}{l!} = 0$. This fact permits neglecting the very high order terms.

In order to analyze the relationship of solution accuracy and the order of a scheme, we assume:

$$f_y^{(l)} = f_y^{(l+1)}. \quad (3)$$

For example, if $f(y) = e^y$, Eq. (3) applies. It is also the case for the linear Burgers equations to be analyzed later in this paper.

First, the variation of maximum truncation error (TE) will be analyzed. For the $(n - m)$ th-order scheme, the TE is defined as

$$TE = f^{(n-m+1)} \max \left(\frac{1}{(n-m+1)!} |D_{n-m+1}| (Re\Delta x)^{n-m+1}, \frac{1}{(n-m+2)!} |D_{n-m+2}| (Re\Delta x)^{n-m+2}, \dots \right).$$

Fig. 1 shows the variation of TE for different order accuracy schemes with different $Re\Delta x$ value (assuming $f^{(n-m+1)} = 1$). It can be seen that with the increased value of $Re\Delta x$, the maximum truncation error of the higher accuracy order scheme is greater than that of the lower accuracy order scheme.

If one of the ending point of the finite differencing stencil in Eq. (1) can be expressed as $f_{i \pm m}$, the truncation error term of a biased upwind differencing after $D_N \frac{1}{N!} f_i^{(N)} (Re\Delta x)^N$ is about $\frac{m Re\Delta x}{N+1}$ times greater than their preceding term in the Taylor's series expansion (again, assuming $f^{(l)} = f^{(l+1)}$), or $\frac{(m Re\Delta x)^2}{(N+1)(N+2)}$ times greater for a central differencing scheme. For example, if $Re\Delta x \leq 2.5$, the terms with $l \geq 11$ can be neglected since they are not dominant. The truncation error before $l = 11$ is defined as

$$R_{10} = f^{(n-m+1)} \sum_{l=n-m+1}^{10} D_l \frac{1}{l!} (Re\Delta x)^l$$

Fig. 2 shows the distribution of R_{10} versus $Re\Delta x$ and indicates that, when $Re\Delta x$ is large, the higher order scheme has higher truncation error. Fig. 3 and Fig. 4 are the zoomed plots of Fig. 2 in different regions. From these two figures, it can be seen that,

- (1). if $Re\Delta x > Re\Delta x|_A \simeq 1.77$, the error of 7th-order scheme is greater than that of 5th-order,
- (2). if $Re\Delta x > Re\Delta x|_B \simeq 1.835$, the error of 7th-order scheme is greater than that of 3rd-order,
- (3). if $Re\Delta x > Re\Delta x|_C \simeq 1.89$, the error of 5th-order scheme is greater than that of 3rd-order,
- (4). if $Re\Delta x > Re\Delta x|_D \simeq 2.08$, the error of the 7th-order, 6th-order, 4th-order schemes are greater than 2th-order central scheme,
- (5). if $Re\Delta x > Re\Delta x|_E \simeq 2.26$, the error of the 5th-order schemes is greater than 2th-order central scheme.
- (6). 3rd-order scheme has the best accuracy if $Re\Delta x > 1.89$.

To solve a convective-diffusive problem, the 2nd-order derivatives need to be discretized. Similar to the first order derivatives, for the approximation of a second order derivative $\frac{\partial^2 f}{\partial x^2}$ at node i (only the central differencing is considered), Taylor series expansion will give

$$\frac{\partial^2 f}{\partial x^2}|_i = \frac{1}{\Delta x^2} \left[\sum_{k=-m}^m c'_k f_{i+k} + \sum_{l=m+1}^{\infty} D'_{2l} \frac{1}{(2l)!} f_i^{(2l)} \Delta x^{2l} \right] \quad (4)$$

Table3 and Table4 give the coefficients c'_k and D'_l of 2nd-, 4th- and 6th-order central differencing schemes, respectively.

Table 3: The coefficients of c'_k

Scheme	f_{i-3}	f_{i-2}	f_{i-1}	f_i	f_{i+1}	f_{i+2}	f_{i+3}
2-order			1	2	1		
4-order		-1/12	16/12	-30/12	16/12	-1/12	
6-order	2/180	27/180	270/180	-490/180	270/180	-27/180	2/180

Table 4: The coefficients of D'_l

Scheme	D'_4	D'_6	D'_8	D'_{10}
2-order	2	2	2	2
4-order		-8	-40	-168
6-order			72	1008

3 Numerical Examples

3.1 Linear Burgers Equation

The linear Burgers equation is usually used as the model equation for Navier-Stokes equation to study the numerical behavior of a scheme.

$$\frac{\partial u}{\partial t} + c \frac{\partial u}{\partial x} = \mu \frac{\partial^2 u}{\partial x^2}, \quad 0 \leq x \leq L \quad (5)$$

Under the boundary conditions:

$$u(0, t) = u_0$$

$$u(L, t) = 0$$

The exact steady state solution of Eq. (5) is

$$u = u_0 \frac{1 - \exp[Re(x/L - 1)]}{1 - \exp(-Re)} \quad (6)$$

where, $Re = \frac{cL}{\mu}$ is the equivalent Reynolds number. The first derivative u'_x can be obtained from Eq.(6) as:

$$u'_x = -\frac{Re}{L} \frac{u_0}{1 - \exp(-Re)} \exp[Re(x/L - 1)] \quad (7)$$

For this linear Burgers equation solution, $u^{(l)} = u^{(l+1)}$, $l = 1, 2, \dots$, and Eq. (3) is satisfied. In this paper, $L = 1$, $c = 1$ and $\mu = 0.01$ are taken and they result in $Re = 10^2$. To measure the accuracy of the numerical solution, we define the absolute error $E = |u'_i - u_i^N|$, where u'_i is the analytical derivative calculated by Eq.(7), u_i^N is the derivative calculated by numerical schemes. Tables 5 and 6 give the absolute errors of different schemes at several locations.

The results in Tables 5 and 6 agree well with the theoretical analysis of section 2. For example, for $Re\Delta x = 1.25$ (Table 5), a high-order scheme obtains a more accurate approximation than a low-order one. When $Re\Delta x$ is increased to 2.5, a lower-order scheme is more accurate(bias-schemes, central schemes).

Table 5: The absolute error $|u'_i - u_i^N|$, $Re\Delta x = 1.25$

Scheme	$x = 0.85$	$x = 0.8625$	$x = 0.875$	$x = 0.8875$
2-order central	8.6122E-6	3.0060E-5	1.0492E-4	3.6620E-4
3-order biased	3.4414E-6	1.2012E-5	4.1924E-5	1.4633E-4
4-order central	2.9972E-6	1.0461E-5	3.6514E-5	1.2745E-4
5-order biased	1.1597E-6	4.0477E-6	1.4128E-5	4.9311E-5
6-order central	1.1284E-6	3.9385E-6	1.3747E-5	4.7981E-5
7-order biased	4.2875E-7	1.4965E-6	5.2233E-6	1.8231E-5

Table 6: The absolute error $|u'_i - u_i^N|$, $Re\Delta x = 2.5$

Scheme	$x = 0.825$	$x = 0.85$	$x = 0.875$	$x = 0.90$
2-order central	3.5658E-6	4.3441E-5	5.2922E-4	6.4472E-3
3-order biased	1.9886E-6	2.4226E-5	2.9513E-4	3.5954E-3
4-order central	6.8302E-6	8.3209E-5	1.0137E-3	1.2349E-2
5-order biased	3.5922E-6	4.3762E-5	5.3313E-4	6.4949E-3
6-order central	1.4512E-5	1.7679E-4	2.1538E-3	2.6238E-2
7-order biased	7.3899E-6	9.0027E-5	1.0968E-3	1.3361E-2

Table 7 gives the comparison of the maximum error and averaged error of all the combinations of the different schemes for the inviscid and viscous terms. For simplicity, the combination of sth -order scheme for convective term and tth -order scheme for diffusive term is named CsDt. It can be seen that if the diffusive term is discretized by a 2nd-order central scheme, the 3rd-order scheme for convective term has the best accuracy for all $Re\Delta x = 2.0, 1.0, 0.5, 0.25$. With the coarse grid ($Re\Delta x = 2.0$), C3D2 outperforms

Table 7: The max error $L_\infty = \text{Max}_i |u_i - u_i^N|$ and averaged error $L_1 = \frac{1}{N} \sum_{i=1}^N |u_i - u_i^N|$

convective scheme, $Re\Delta x$		diffusive (2nd)		diffusive (4th)		diffusive (6th)	
		L_∞	L_1	L_∞	L_1	L_∞	L_1
2nd	2.00	0.1353E+00	0.3069E-02	0.2999E+00	0.7412E-02	0.1618E+00	0.4120E-02
	1.00	0.3455E-01	0.8116E-03	0.6478E-01	0.1654E-02	0.5759E-01	0.1510E-02
	0.50	0.7879E-02	0.2064E-03	0.1540E-01	0.4082E-03	0.1503E-01	0.3982E-03
	0.25	0.1929E-02	0.5188E-04	0.3807E-02	0.1026E-03	0.3777E-02	0.1017E-03
3rd	2.00	0.8318E-02	0.2161E-03	0.1511E+00	0.4144E-02	0.4423E-01	0.1235E-02
	1.00	0.8645E-02	0.2172E-03	0.2262E-01	0.6087E-03	0.1763E-01	0.4852E-03
	0.50	0.4383E-02	0.1169E-03	0.3253E-02	0.8766E-04	0.2980E-02	0.8023E-04
	0.25	0.1470E-02	0.3974E-04	0.4401E-03	0.1190E-04	0.4228E-03	0.1142E-04
4th	2.00	0.3593E+00	0.8203E-02	0.1587E+00	0.3881E-02	0.2720E+00	0.6816E-02
	1.00	0.4705E-01	0.1089E-02	0.8645E-02	0.2172E-03	0.1299E-01	0.3352E-03
	0.50	0.8371E-02	0.2227E-03	0.5043E-03	0.1353E-04	0.7597E-03	0.2032E-04
	0.25	0.1957E-02	0.5290E-04	0.3181E-04	0.8785E-06	0.4750E-04	0.1303E-05
5th	2.00	0.2003E+00	0.4965E-02	0.3772E-01	0.9882E-03	0.1428E+00	0.3813E-02
	1.00	0.3494E-01	0.8456E-03	0.1713E-03	0.4480E-05	0.4587E-02	0.1222E-03
	0.50	0.7669E-02	0.2044E-03	0.9445E-04	0.2527E-05	0.1613E-03	0.4347E-05
	0.25	0.1909E-02	0.5163E-04	0.1007E-04	0.2642E-06	0.5745E-05	0.1734E-06
6th	2.00	0.1709E+00	0.4094E-02	0.3199E+00	0.7863E-02	0.1925E+00	0.4836E-02
	1.00	0.2927E-01	0.6755E-03	0.7059E-02	0.1767E-03	0.2151E-02	0.5526E-04
	0.50	0.7476E-02	0.2005E-03	0.2878E-03	0.7740E-05	0.3027E-04	0.8029E-06
	0.25	0.1907E-02	0.5157E-04	0.1603E-04	0.4241E-06	0.2182E-06	0.1793E-07
7th	2.00	0.2208E-01	0.5379E-03	0.1708E+00	0.4398E-02	0.5838E-01	0.1533E-02
	1.00	0.2989E-01	0.7129E-03	0.4895E-02	0.1257E-03	0.2516E-03	0.6607E-05
	0.50	0.7487E-02	0.2003E-03	0.2542E-03	0.6833E-05	0.2139E-05	0.7694E-07
	0.25	0.1904E-02	0.5151E-04	0.1545E-04	0.4085E-06	0.4479E-06	0.2856E-07

all other schemes, higher or lower order. This shows that the higher order scheme does not necessarily generate better results. When $Re\Delta x \leq 1.0$, all the high order schemes are more accurate. This confirms the analytical conclusion of section 2.

Figs. 5 and 6 are the comparison of numerical results with $Re\Delta x = 2.0$. It can be seen that the 3rd-order biased scheme obtains the most accurate solution. The 2nd-order central scheme and 6th-order central scheme for convective term obtain oscillatory results. This also indicates that the biased upwind schemes are preferred for convective-diffusive problem due to the hyperbolic characteristics of the governing equation. Note the maximum errors of the high order schemes occur in the high gradient variation (2nd order derivative) region, i.e., $x = 0.93 - 0.97$.

3.2 Nonlinear Burgers Equation

The nonlinear Burgers equation:

$$\frac{\partial u}{\partial t} + u \frac{\partial u}{\partial x} = \mu \frac{\partial^2 u}{\partial x^2}, \quad -1 \leq x \leq L \quad (8)$$

usually serves as the model equation for the Navier-Stokes equation with nonlinear convective terms. The exact steady state solution of Eq. (8) is

$$u = \tanh(-Re x/2)$$

under the boundary conditions

$$u(-1, t) = \tanh(Re/2)$$

$$u(L, t) = \tanh(-LRe/2)$$

where, $Re = \frac{1}{\mu}$ is the equivalent Reynolds number. For this case, $\mu = 0.01$ and $L = 0$ are used. The first derivative u'_x is

$$u'_x = -\frac{Re}{2} \frac{1}{ch^2(-Re x/2)} \quad (9)$$

For this nonlinear Burgers equation, there is no clear relation satisfying Eq. 3. Hence the criterion $Re\Delta x \leq 1$ may not strictly apply. We hence hope to gain more hints from the numerical experiments.

Tables 8, 9 and 10 give the absolute errors of different schemes at several locations. For this example, since

$$u^{(l)} = Re^l f_y^{(l)}(Re x),$$

it may need a more strict $Re\Delta x$ to ensure a high-order scheme achieving more accurate approximation than a low-order scheme. From Table 8, it can be seen that, even at $Re\Delta x = 1$, the 6th-order scheme has the largest error whereas the 3rd-order scheme has the smallest error.

Table 8: The absolute error $|u'_i - u_i'^N|$, $Re\Delta x = 1.0$

Scheme	$x = -0.07$	$x = -0.06$	$x = -0.05$	$x = -0.04$
2-order central	2.7055E-4	1.9990E-3	1.4762E-2	0.1086
3-order biased	1.3815E-4	1.0207E-3	7.5370E-3	5.5407E-2
4-order central	2.8477E-4	2.1028E-3	1.5461E-2	0.1101
5-order biased	1.3850E-4	1.0225E-3	7.5110E-3	5.3116E-2
6-order central	3.2848E-4	2.4122E-3	1.7022E-2	8.7927E-2
7-order biased	1.5545E-4	1.1403E-3	7.9801E-3	3.7994E-2

Table 9: The absolute error $|u'_i - u_i'^N|$, $Re\Delta x = 1.25$

Scheme	$x = -0.15$	$x = -0.1375$	$x = -0.125$	$x = -0.1125$
2-order central	5.3155E-11	6.4754E-10	7.8888E-9	9.6105E-8
3-order biased	2.9627E-11	3.6111E-10	4.3994E-9	5.3596E-8
4-order central	1.0182E-11	1.2404E-9	1.5111E-8	1.8409E-7
5-order biased	5.3542E-11	6.5236E-10	7.9472E-9	9.6817E-8
6-order central	2.1632E-10	2.6353E-9	3.2105E-8	3.9112E-7
7-order biased	1.1016E-10	1.3420E-9	1.6349E-8	1.9917E-7

Table 11 gives the comparison of maximum error and averaged error between the exact steady state solutions and numerical solutions. For cases of $Re\Delta x = 2.5, 2, 1$ with 2nd-order central scheme for diffusive term, the 3rd-order biased scheme is again the most accurate. Even for $Re\Delta x = 2$, only the results of C5D4 and C7D6 are more accurate than C3D2. However, when $Re\Delta x \leq 1.0$, all the high order schemes

Table 10: The absolute error $|u'_i - u'^N_i|$, $Re\Delta x = 2.5$

Scheme	$x = -0.1725$	$x = -0.15$	$x = -0.125$	$x = -0.10$
2-order central	3.4769E-12	5.1806E-10	7.6887E-8	1.1411E-5
3-order biased	2.2557E-12	3.3662E-10	4.9957E-8	7.4143E-6
4-order central	8.7863E-11	1.3038E-8	1.9350E-6	2.8716E-4
5-order biased	5.2061E-11	7.7241E-9	1.1464E-6	1.7013E-4
6-order central	2.5869E-9	3.8393E-7	5.6978E-5	8.3966E-3
7-order biased	1.4635E-9	2.1721E-7	3.2235E-5	4.7500E-3

have more accurate results. This is similar to the criterion drawn from the linear Burgers equation.

Figs. 7 and 8 are the comparison of numerical results with $Re\Delta x = 2.0$, which show that the discrepancy primarily occurs in the region with large gradient variation (2nd order derivative).

3.3 Wall Boundary Layer

The accuracy of different order schemes for wall boundary layer flows is certainly of great interest to CFD researchers. A steady state laminar supersonic boundary layer flow on an adiabatic flat plate is hence calculated to examine this issue.

For a compressible boundary layer, we may use the following transformation[2]

$$\eta = y \sqrt{\frac{ReU}{2x}} = Ay \quad (10)$$

where

$$\begin{aligned} A &= \sqrt{\frac{ReU}{2x}} \\ u &= U f'(\eta) \end{aligned} \quad (11)$$

The grid Reynolds number is defined as

$$Re_{\Delta y} = \frac{\rho_i u_i \Delta y_i}{\mu_i}$$

For the numerical solution, the 2D-normalized compressible full Navier-Stokes equations are solved.

The incoming Mach number is 2.0. The Reynolds number based on the length of the flat plate is 1.0×10^5 . The Prandtl number of 1.0 is used in order to compare with the analytical solution. The computation domain is taken to be $[0, 2] \times [0, 1.6]$. The CFL number of 200 is used in all calculations. All the calculations are converged to machine zero with the residual less than 10^{-12} by using the implicit time marching method with unfactored Gauss-Seidel line relaxation[3, 4, 5].

Four meshes of 180×80 , 180×160 , 180×320 , and 180×640 are used. The baseline mesh size 180×80 is stretched near wall surface. The refined meshes are then generated by reducing the mesh spacing by half in y-direction and the mesh size becomes $180 \times (n \times 80)$, $n = 2, 3, 4$. Fig. 9 is the mesh sketch.

The Roe's flux difference scheme[6] is used as the Riemann solver with the 3rd-order, 5th-order and 7th-order reconstruction for the conservative variables. The viscous terms are discretized by 2nd-order, 4th-order[7] and 6th-order[8] central schemes. In all plots, 'CsDt' denotes 's'th-order scheme for inviscid terms and 't'th-order scheme for viscous terms.

Table 11: The max error $L_\infty = \text{Max}_i |u_i - u_i^N|$ and averaged error $L_1 = \frac{1}{N} \sum_{i=1}^N |u_i - u_i^N|$

convective scheme, $Re\Delta x$		diffusive (2nd)		diffusive (4th)		diffusive (6th)	
		L_∞	L_1	L_∞	L_1	L_∞	L_1
2nd	2.50	0.2429E-01	0.1174E-02	0.4562E-01	0.2223E-02	0.4851E-01	0.2442E-02
	2.00	0.2954E-01	0.1042E-02	0.4844E-01	0.1726E-02	0.5024E-01	0.1828E-02
	1.00	0.1263E-01	0.2818E-03	0.2031E-01	0.5050E-03	0.2048E-01	0.5150E-03
	0.50	0.3166E-02	0.7113E-04	0.5781E-02	0.1357E-03	0.5799E-02	0.1356E-03
3rd	2.50	0.2143E-02	0.1159E-03	0.1567E-01	0.8896E-03	0.1882E-01	0.1057E-02
	2.00	0.2700E-02	0.8322E-04	0.1490E-01	0.5858E-03	0.1765E-01	0.7001E-03
	1.00	0.1084E-01	0.1723E-03	0.4112E-02	0.9327E-04	0.3973E-02	0.9335E-04
	0.50	0.3721E-02	0.6677E-04	0.1247E-02	0.2199E-04	0.1062E-02	0.2050E-04
4th	2.50	0.2272E-01	0.9611E-03	0.1052E-01	0.4182E-03	0.1657E-01	0.6949E-03
	2.00	0.1361E-01	0.4707E-03	0.1185E-01	0.4606E-03	0.1557E-01	0.6080E-03
	1.00	0.7100E-02	0.2084E-03	0.3171E-02	0.5792E-04	0.4111E-02	0.7757E-04
	0.50	0.2805E-02	0.6626E-04	0.2420E-03	0.4680E-05	0.3471E-03	0.6810E-05
5th	2.50	0.2419E-01	0.1098E-02	0.5074E-02	0.1666E-03	0.6054E-02	0.2437E-03
	2.00	0.1955E-01	0.7288E-03	0.1073E-02	0.3705E-04	0.4924E-02	0.1704E-03
	1.00	0.1276E-01	0.2513E-03	0.1859E-02	0.3652E-04	0.1276E-02	0.2606E-04
	0.50	0.3048E-02	0.7117E-04	0.5193E-03	0.4310E-05	0.3807E-03	0.4004E-05
6th	2.50	0.3366E-01	0.1769E-02	0.1042E-01	0.4303E-03	0.5771E-02	0.2854E-03
	2.00	0.2400E-01	0.8739E-03	0.3304E-02	0.1570E-03	0.6169E-02	0.2406E-03
	1.00	0.1079E-01	0.2652E-03	0.7971E-03	0.1668E-04	0.1198E-02	0.2585E-04
	0.50	0.3174E-02	0.7043E-04	0.8497E-04	0.1726E-05	0.4145E-04	0.6401E-06
7th	2.50	0.3079E-01	0.1577E-02	0.1143E-01	0.5514E-03	0.7592E-02	0.2804E-03
	2.00	0.2449E-01	0.9338E-03	0.4942E-02	0.1957E-03	0.1495E-02	0.4153E-04
	1.00	0.1293E-01	0.2614E-03	0.1880E-02	0.3583E-04	0.8347E-03	0.1677E-04
	0.50	0.3063E-02	0.7103E-04	0.2977E-03	0.2586E-05	0.1751E-03	0.1792E-05

The comparison of results are plotted in Figs. 10-13. For the plot of the whole velocity profiles, the difference between different schemes is not distinguishable by eyes (see Figs. 10, 12 and 14). But the corresponding zoomed plot can display the accuracy difference of different schemes as shown in 11, which is the zoomed plot of Fig. 10 in the region of $\eta = 2.47$ with high 2nd order derivative of the velocity. It indicates that for the mesh of 180×80 , C3D2 is the most accurate, then followed by C5D2, C7D2, C3D4, C3D6, C5D4, C5D6, C7D4 and C7D6, respectively. The lower-order scheme obtains more accurate results than the higher-order schemes, for both the inviscid terms and viscous terms.

For the one level refined mesh of 180×160 as shown in Fig. 13, the better accuracy sequence is C3D2, C5D2, C7D2, C3D6, C5D6, C3D4, C5D4, C7D6, C7D4. In this case, for the 5th-order and 7th-order inviscid schemes, the 6th-order central scheme for viscous terms gives better result than the 4th-order central scheme.

With the further refined mesh of 180×320 (Fig. 15), the most accurate scheme is C5D4, then followed by C3D6, C7D6, C5D4, C7D4, C5D6, C3D2, C7D2. In this case, the 5th-order scheme is more accurate than the 3rd-order scheme, the 3rd-order scheme is still better than 7th-order scheme. For the viscous terms, higher-order scheme obtains more accurate results.

Fig. 16 is the comparison of grid convergence. The result of mesh 180×320 is virtually identical to that of mesh 180×640 . They all agree excellently with the Blasius solution. Fig. 16 shows that the improvement with the refined mesh is mostly in the region near the boundary layer edge, where the velocity

gradient variation or the 2nd order derivative of velocity is the maximum.

Fig. 17 is the plot of grid Reynolds number. In the region $2 \leq \eta \leq 4$, the velocity gradient or the 2nd order derivative of velocity varies largely, the grid Reynolds number is below 25 with the finest mesh of 180×640 , which gives the best results. Hence, for the calculation of laminar boundary layer, it maybe recommended to keep the grid Reynolds number less than 25 across the boundary layer. However, this is not the mesh size criterion that a higher order scheme will be more accurate than a lower scheme. It is just the mesh spacing to accurately resolve the wall profile for all the schemes.

Due to the time constraint, we have not found the best mesh spacing criterion yet for Navier-Stokes equation so that a higher order scheme will be more accurate than a lower order scheme. The criterion of the linear Burgers equation $Re\Delta x \leq 1$ may be preventively expensive. The study of this criterion is in progress and we hope to report it in future.

3.4 Conclusion

This paper investigates different high order finite difference schemes and their accuracy for Burgers equation and Navier-Stokes equations. On a coarse grid, theoretical and numerical analysis indicate that a higher order difference scheme does not necessarily obtain more accurate solutions than a lower order scheme in the regions of high gradient variation (2nd order derivative). It is because the truncation error of a finite differencing scheme depends on $Re\Delta x$ instead of just Δx if the solution is an exponential function as that of the linear Burgers equation. On a coarse grid, the numerical experiments indicate that the 3rd order biased upwind differencing for the inviscid fluxes with 2nd order central differencing for viscous term outperforms all other schemes with the accuracy order as high as 7th order.

For the linear Burgers equation, both the analytical and numerical results indicate that a higher order scheme will be more accurate than a lower order scheme only when the product of Reynolds number and the mesh size is less than 1, i.e., $Re\Delta x \leq 1$. For the nonlinear Burgers equation, the numerical experiments also show the same conclusion even though a clear analytical conclusion is difficult to obtain.

A laminar wall boundary layer solution obtained by solving Navier-Stokes equations is used as the example for different order schemes, which shows the same observation that the 3rd order biased upwind differencing with a 2nd order central differencing is the most accurate on a coarse grid. A higher order scheme does not necessarily give a more accurate solution unless the mesh is sufficiently fine. The conception that a high order scheme can save mesh size unconditionally may be incorrect. Since the discrepancy occurs mostly in the region with high gradient variation near the edge of a boundary layer, to accurately resolve a wall boundary layer, the refined mesh should not only be near the wall surface where the gradient is high, but also near the edge of the boundary layer where the gradient variation is high.

The mesh spacing criterion for Navier-Stokes equation that a higher order scheme will be more accurate than a lower order scheme is not obtained yet due to the time limit to submit this paper. Using the criterion of the linear Burgers equation $Re\Delta x \leq 1$ for Navier-Stokes equations may be excessive and preventively expensive. The study of this criterion is in progress and we hope to report it in future. To resolve the laminar wall boundary layer accurately, the recommended grid Reynolds number is to be below 25 across the boundary layer. However, this is the criterion from the numerical experiments for all the finite differencing schemes, not for a higher order schemes to have better accuracy than a lower order scheme.

4 Acknowledgment

This work is supported by AFOSR Grant FA9550-06-1-0198 monitored by Dr Fariba Fahroo, and is supported by Miami Wind TM at University of Miami.

References

- [1] J. A. Ekaterinaris, “High-order accurate, low numerical diffusion methods for aerodynamics,” *Progress in Aerospace Sciences*, vol. 41, pp. 192–300, 2005.
- [2] F. M. White, *Viscous Fluid Flow, 2nd edition*. McGraw-Hill, Inc, 1991.
- [3] Z. Hu, G. -C Zha, “Calculations of 3D compressible using an efficient low diffusion upwind scheme,” *International Journal for Numerical Methods in Fluids*, vol. 47, pp. 253–269, 2005.
- [4] Z. J. Hu, “Parallel computation of fluid-structural interactions using high resolution upwind schemes.” Ph.D. Thesis, Dept. of Mech. Aero. Eng., Univ. of Miami, May 2005.
- [5] X. Chen, G. -C Zha, “Fully coupled fluid-structural interactions using an efficient high solution upwind scheme,” *Journal of Fluid and Structure*, vol. 20, pp. 1105–1125, 2005.
- [6] P. Roe, “Approximate Riemann Solvers, Parameter Vectors, and Difference Schemes,” *Journal of Computational Physics*, vol. 43, pp. 357–372, 1981.
- [7] Y. Q. Shen, G.-Z. Zha, X. Y. Chen, “High Order Conservative Differencing for Viscous Terms and the Application to Vortex-Induced Vibration Flows.” AIAA Paper 2008-4059, AIAA 38th Fluid Dynamics Conference and Exhibit, Seattle, Washington, Jun 2008.
- [8] Y. Q. Shen, G. -C. Zha, “Comparison of High Order Schemes for Large Eddy Simulation of Circular Cylinder Flow.” accepted by the 47th AIAA Aerospace Sciences Meeting, AIAA-2009-0945, Jan 2009.

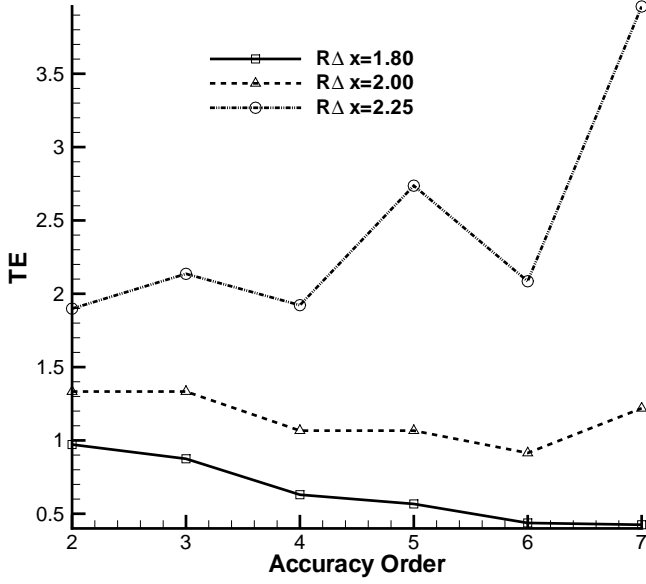


Figure 1: The variation of maximum truncation error vs order of accuracy assuming $f^{(n-m+1)} = 1$

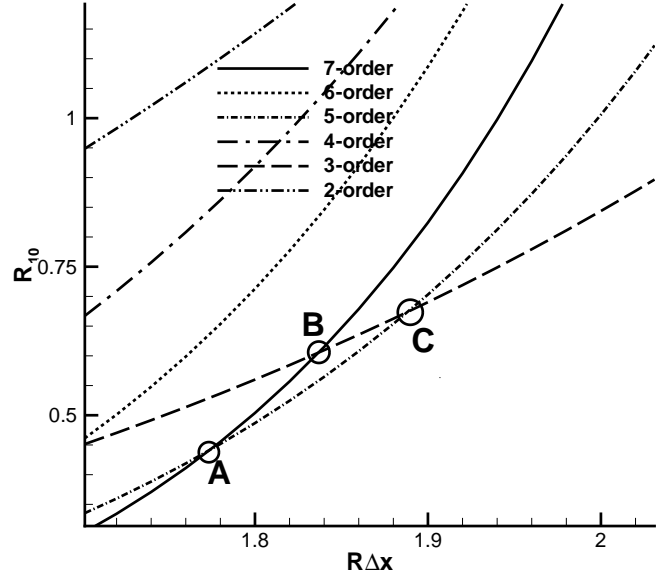


Figure 3: The zoomed plot of Fig. 2, the truncation error Re_{10} vs $Re\Delta x$

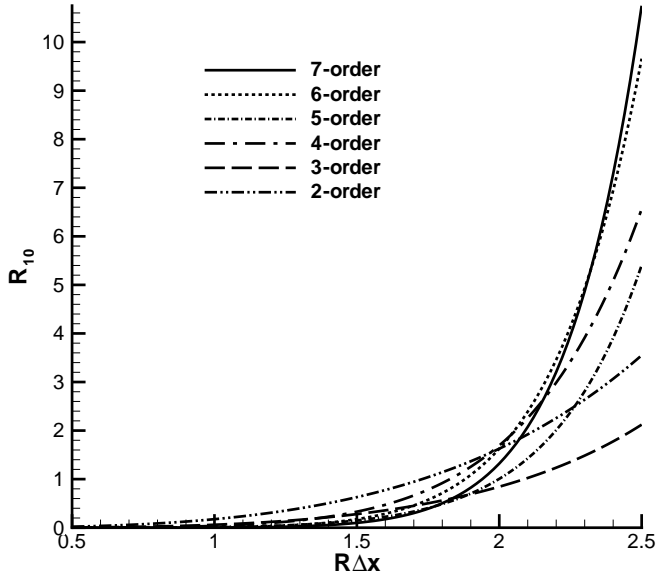


Figure 2: The truncation error Re_{10} vs $Re\Delta x$

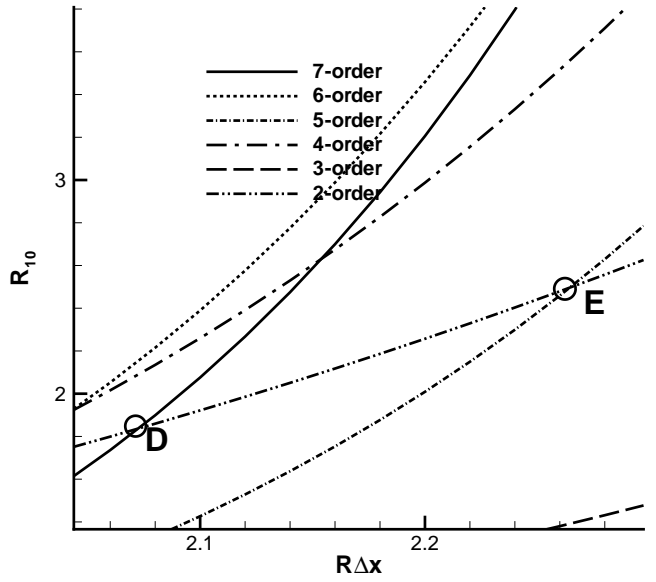


Figure 4: The zoomed plot of Fig. 2, the truncation error Re_{10} vs $Re\Delta x$

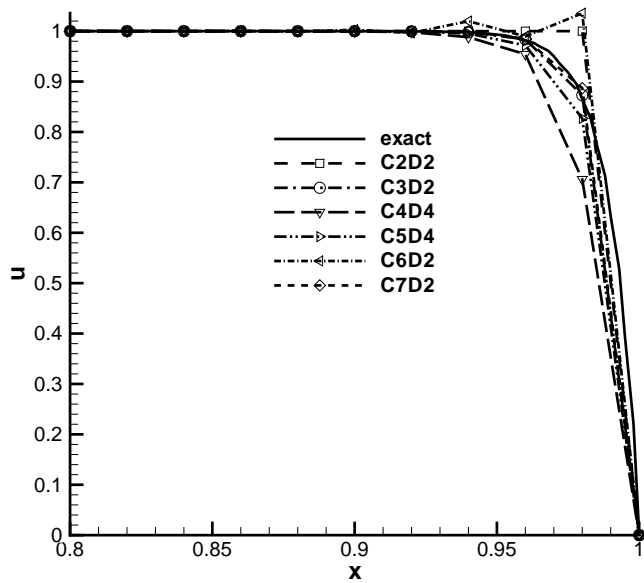


Figure 5: Comparison of the solutions of the linear Burgers equation using different order of numerical schemes

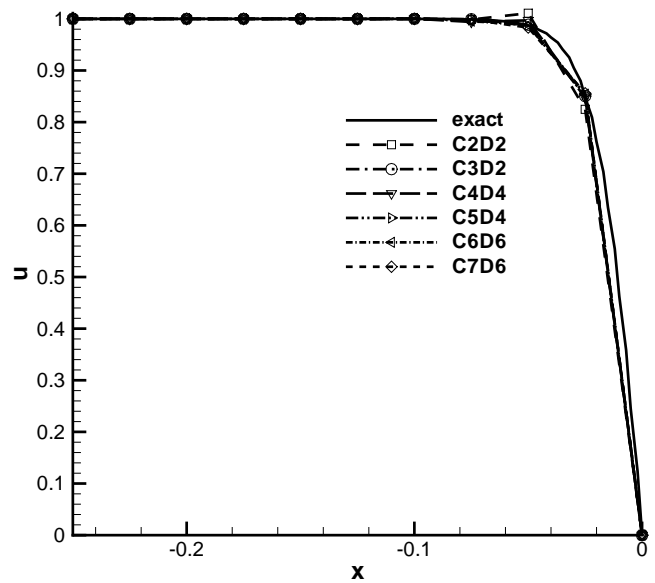


Figure 7: Comparison of the solutions of the nonlinear Burgers equation using different order of numerical schemes

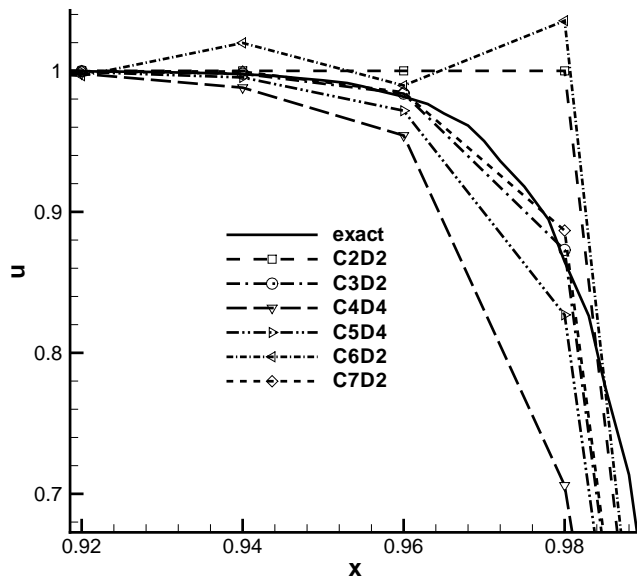


Figure 6: Zoomed plot of Fig. 5, the solutions of the linear Burgers equation using different order of numerical schemes

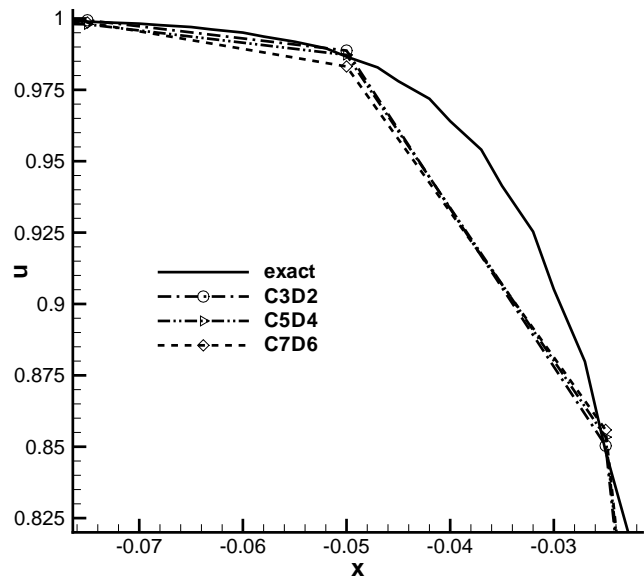


Figure 8: Zoomed plot of Fig. 7, the solutions of the nonlinear Burgers equation using different order of numerical schemes

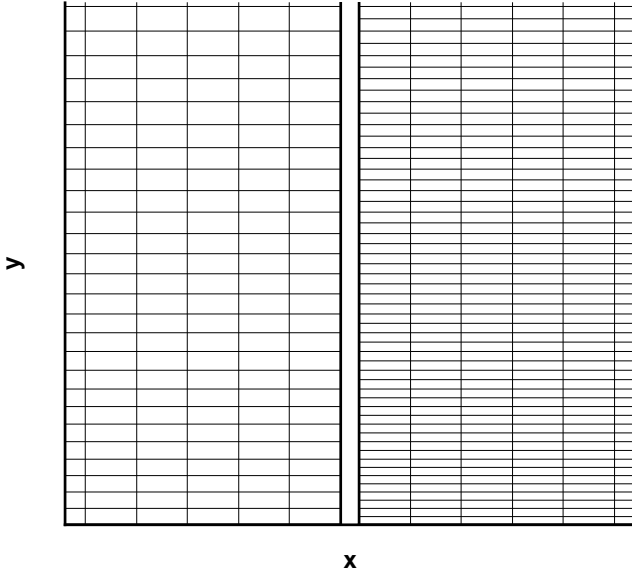


Figure 9: Mesh sketch. Left: coarse mesh of 180×160 . Right: refined mesh of 180×320

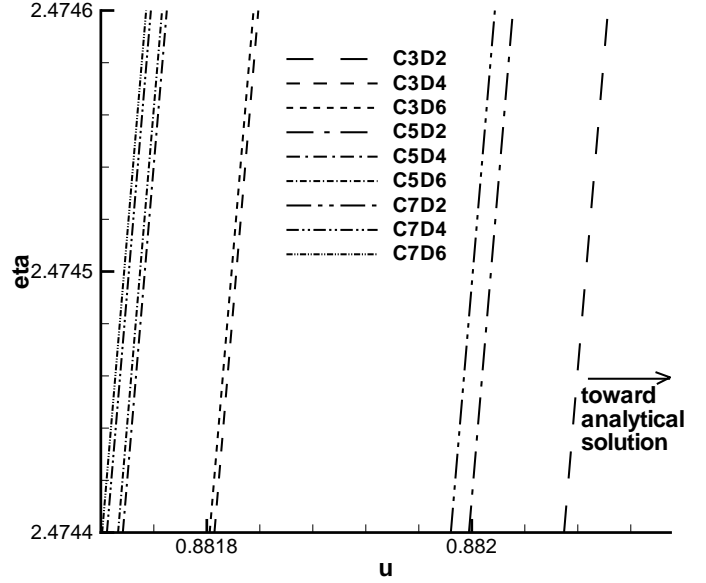


Figure 11: Zoomed plot of Fig. 10, Velocity profiles calculated using different order of numerical schemes with baseline mesh.

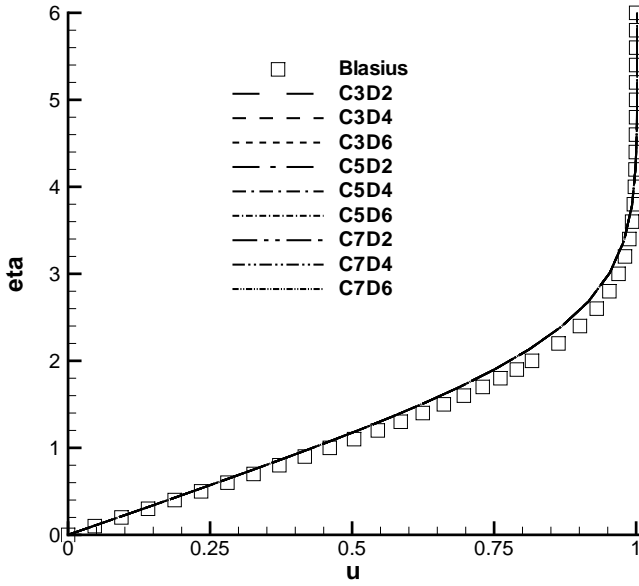


Figure 10: Velocity profiles calculated using different order of numerical schemes with baseline mesh.

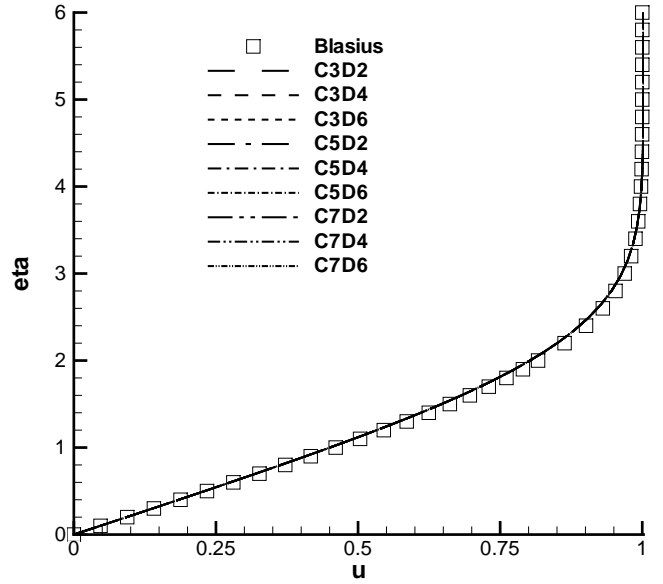


Figure 12: Velocity profiles calculated using different order of numerical schemes with one level refined mesh 180×160 .

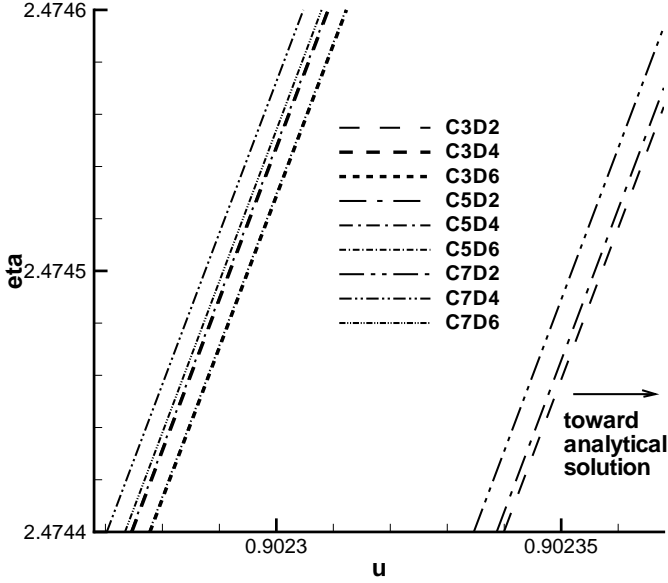


Figure 13: Zoomed plot of Fig. 12, velocity profiles calculated using different order of numerical schemes with one level refined mesh 180×160 .

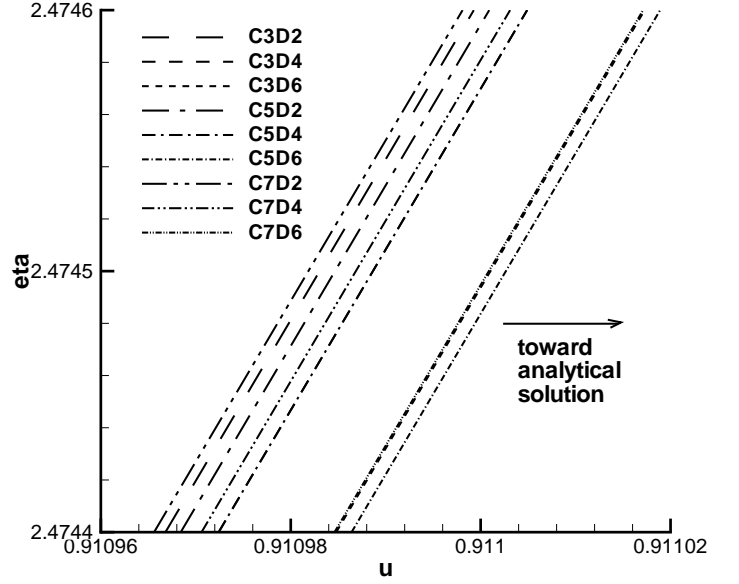


Figure 15: Zoomed plot of Fig. 14, velocity profiles calculated using different order of numerical schemes with two level refined mesh 180×320

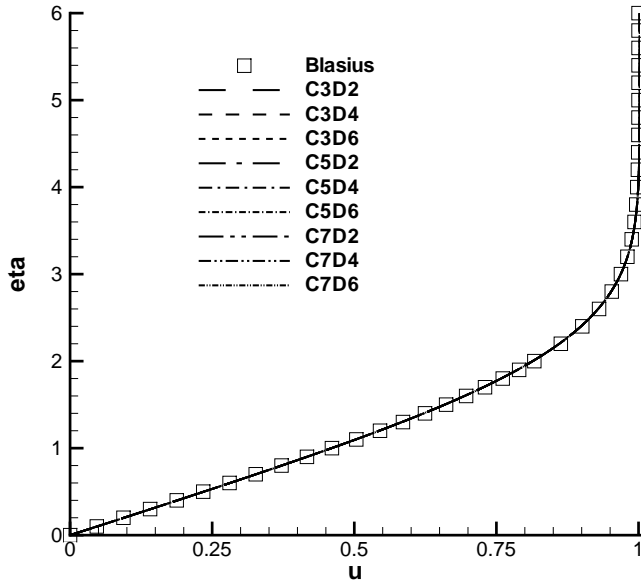


Figure 14: Velocity profiles calculated using different order of numerical schemes with two level refined mesh 180×320

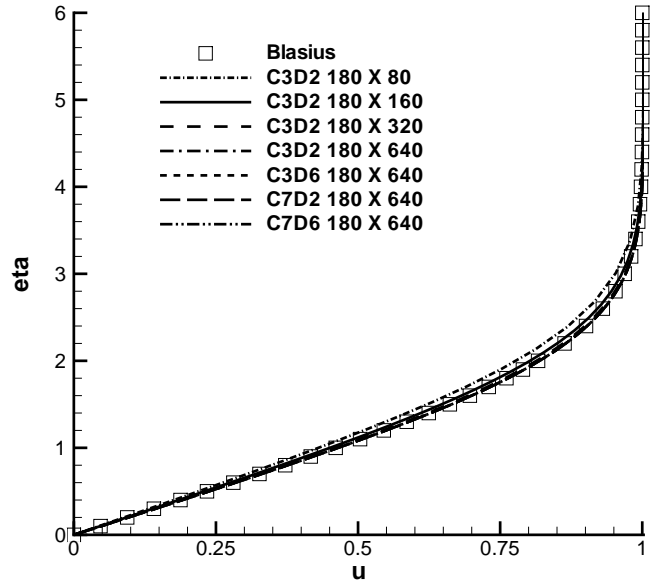


Figure 16: Comparison of grid convergence for the velocity profiles

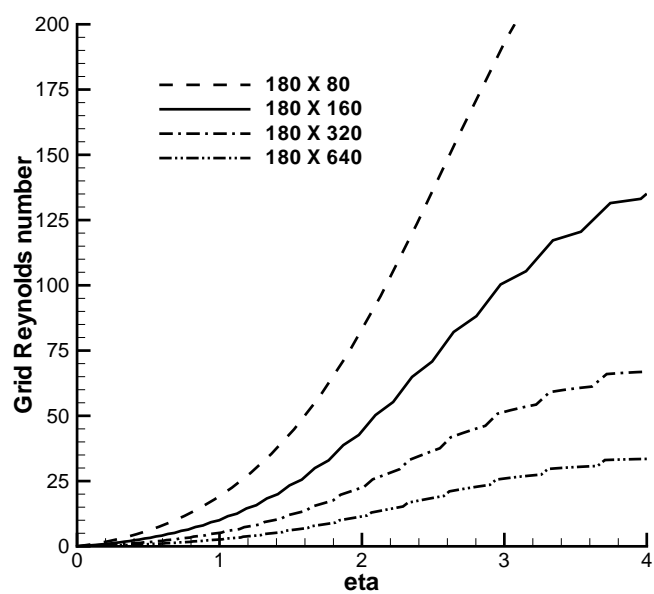


Figure 17: Comparison of grid Reynolds number for different mesh sizes